ACS Energy LETTERS

http://pubs.acs.org/journal/aelccp

Ultrafast Reaction Mechanisms in Perovskite Based Photocatalytic C−C Coupling

Kang Wang,[#] Haipeng Lu,[#] Xiaolin Zhu,[#] Yixiong Lin, Matthew C. Beard,[*] Yong Yan,[*] and Xihan Chen[*]

Cite This: *ACS Energy Lett.* 2020, 5, 566−571

Read Online

ACCESS | Metrics & More | Article Recommendations | Supporting Information

ABSTRACT: **Solar driven carbon−carbon (C−C) bond formation is a new direction in solar energy utilization. Earth abundant nanocrystal based photocatalysts are highly sought after as they can potentially eliminate expensive noble metal catalysts. A detailed understanding of the underlying reaction mechanisms could provide guidance in designing new systems that can activate a larger class of small molecules. Here, we employ transient absorption spectroscopy to study a model C−C bond formation reaction, i.e., α-alkylation of aldehydes catalyzed by colloidal $CsPbBr_3$ nanocrystals (NCs). We find that both electrons and holes undergo ultrafast charge transfer (∼50 ps) from photoexcited perovskite NCs to reactant molecules. A charge separated state lives for more than 0.8 μs, enabling a radical mechanism to form the C−C bonds. We discuss the differences between the NCs photoredox catalysts and the molecular catalyst.**

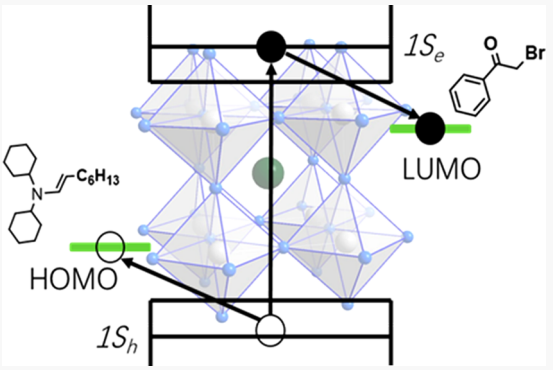

Photocatalysis using solar energy has long been of interest to the chemistry community.[1−3] In general, photoexcitation creates electron−hole pairs that can then subsequently transfer (electron/hole/energy) to reactants to initiate a reaction. A subsequent hole/electron transfer returns the catalyst to its original state, completing the catalytic cycle (if initiated by charge transfer mechanism).[4−6] The development of new efficient photocatalytic systems requires knowledge from many areas of chemistry and physics, including design, synthesis, characterizations, and mechanistic understanding, so as to direct the solar energy into desired products with little loss. The understanding of charge-carrier dynamics and reaction kinetics provide key insights in designing and synthesizing new systems.[7,8]

Apart from highly desired solar driven CO_2 reduction[9] and water splitting[10,11] to generate fuels, producing valuable organic products using sunlight driven photoredox catalysis is receiving attention. Pioneering work by MacMillan[12] and Yoon[13] have shown successful photodriven carbon−carbon (C−C) bond formation, a fundamental transformation of organic synthesis using Ru molecular based photocatalyst. Recently, perovskite nanocrystals (NCs) are being explored[14−16] as an alternative to photocatalyze such C−C bond formation reactions under visible light. The advantage of perovskite NCs is that product separation should be easier and the elimination of the expensive noble metal molecular catalysts.[12,17,18] In addition to the charge transfer mechanism, perovskites NCs can also promote efficient and rapid energy transfer to organic substrates, generating long-lived molecular triplets that can initiate photocatalytic reactions.[19−22] NCs surfaces can support different catalytic mechanisms and thus offer a new type of photocatalyst with different reaction mechanisms allowing for greater tunability in targeted reactions.

The reaction mechanisms for NCs based photocatalytic systems are fundamentally interesting as the charge transfer/recombination dynamics are of crucial importance in the design of new photocatalytic systems that can activate a larger class of small molecules.[23,24] Recent studies by Weix[5] and Weiss[25] have demonstrated the use of transient absorption spectroscopy to investigate reaction dynamics/mechanism in CdSe NCs based photocatalytic systems. Ideally, the initial charge transfer should be fast (efficient) and result in long-lived intermediates that can take part in diffusion-controlled reactions, while deleterious charge recombination needs to be slow so that subsequent steps of the reaction can occur prior to deactivation of the catalyst. The lifetime of the photoexcited

Received: December 13, 2019
Accepted: January 21, 2020
Published: January 22, 2020

https://dx.doi.org/10.1021/acsenergylett.9b02714
ACS Energy Lett. 2020, 5, 566−571

catalyst can also dictate the specific reaction mechanism (*vida infra*).

We employ transient absorption (TA) spectroscopy to investigate the charge transfer and reaction dynamics of a model $CsPbBr_3$ NCs photocatalytic system. We study the reaction between 2-bromoacetophenone and octanal with dicyclohexylamine as a cocatalyst and 2,6-lutidine as a base (Figure 1c). We find an ultrafast electron transfer process that

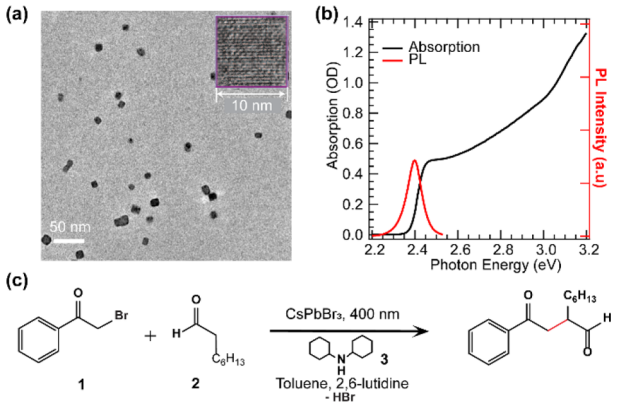

Figure 1. (a) TEM image of the as-synthesized $CsPbBr_3$ NCs. The size of the NCs are close to 10 nm. The inset of (a) shows a high-resolution TEM image of one synthesized NC. (b) Linear absorption and PL spectrum of $CsPbBr_3$ NCs. The absorption onset and the center of the PL peak is near 2.4 eV. (c) Reaction scheme of the α-alkylation catalyzed by $CsPbBr_3$ NCs.

occurs from $CsPbBr_3$ NCs to 2-bromoacetophenone and a hole transfer to an *in-situ* formed enamine (formed via dicyclohexylamine and octanal) or cocatalyst. In each case the ET (electron transfer) or HT (hole transfer) is followed by a ~0.8/0.5 μs charge separation time. The microsecond charge separation time is needed for the formation of C−C bonds and is thus the limiting factor. The efficient ET and HT from perovskite NCs confirm their great potential in organic photocatalysis.

Colloidal $CsPbBr_3$ NCs are synthesized using an amine-free method[19] (see the Supporting Information). Note that we employ amine-free NCs, designed here, to avoid any possible charge transfer (CT) to the ligand-capping amine, so that we only focus on the CT dynamics for the desired organic reaction. The average size of the NCs are ~10 nm, as measured by TEM (Figure 1a and Figure 1a inset), and they crystallize in the orthorhombic phase similar to results in previous reports.[26] The as-synthesized NCs are characterized by UV−vis absorption and photoluminescence (PL) spectra (Figure 1b). The onset of absorption corresponds to a bandgap of ~2.4 eV. The as-prepared perovskite NCs are directly employed in the photocatalytic α-alkylation reaction (Figure 1c).

To verify that the NCs serve as photocatalysts, the reaction should be triggered by light that is only absorbed by the NCs and not by any other reagents in the reaction mixture. The absorption spectra of the above reaction mixtures are dominated by the NCs for photon energies ranging from 2.4 to 3.2 eV, as indicated by the invariance of the absorption spectra (Figure 2a). Therefore, we employed excitation light with 3.1 eV (400 nm) in the subsequent transient absorption (TA) experiments to ensure only excitation of the NCs. The probe light in the TA study consists of a white-light continuum pulse with photon energies that span 1.6−2.8 eV (see the

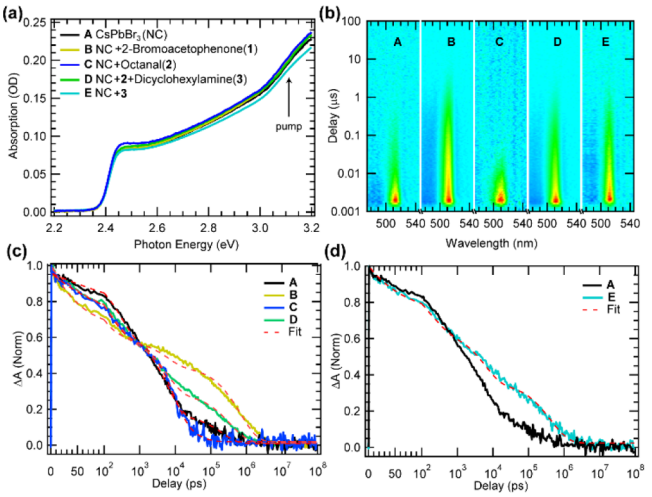

Figure 2. (a) Linear absorption spectrum of A (pure NCs), B (NCs + 2-bromoacetophenone (1)), C (NCs + octanal (2)), D (NCs + octanal (2) + dicyclohexylamine (3)), and E (NCs + dicyclohexylamine (3)). The absorption spectrum is dominated by absorption of the $CsPbBr_3$ NCs. (b) Pseudocolor image plot of the TA experiments of A−E in toluene. The *y*-axis indicates pump−probe delay time, and the *x*-axis indicates the probe wavelength. The bright red color corresponds to a photoinduced NCs exciton ground state bleach while blue is a photoinduced absorption. (c) Normalized TA kinetics probed at the center of the NCs exciton bleach spectrum for A−D. Red-dashed traces are fits to kinetics. (d) Normalized TA kinetics and fits for A and E. (Also see Figure S1 for a comparison between D and E.)

Supporting Information). In all TA experiments discussed below, the excitation power density was controlled so that only ~0.06 excitons per NC (see the Supporting Information) are produced. Therefore, the TA signals are dominated by NCs that have only absorbed one photon.[27,28]

Figure 2b shows typical pseudocolor image plots of the TA experiments for each sample suspended in toluene. The *y*-axis indicates the pump−probe delay time, and the *x*-axis indicates the probe wavelength. The color indicates the intensity of the photoinduced absorption (PIA) or photoinduced ground state bleach (GSB). The GSB dynamics can be followed to monitor the reaction progress.[29,30] In the pseudocolor image, the bright red color corresponds to the photoinduced GSB of the NCs. Figure 2c shows the normalized TA kinetics probed at the center of the NCs GSB. Samples **A**, **B**, **C**, and **D** where NCs with individual reactants and cocatalyst are plotted. For **A**, the isolated NCs, the dynamics of the exciton decay is similar to what has been reported and exhibits exciton recombination dynamics that are multiexponential.[27,31]

Compared with the dynamics for isolated NCs, the dynamics for **B** (NCs + 2-bromoacetophenone (**1**)) show an initial faster decay of around 50 ps followed by a much slower decay in the μs time frame. Such behavior is characteristic of an ultrafast charge transfer followed by a long-lived charge separated state.[32] In contrast, for **C** (NCs with octanal (**2**)), the transient kinetics only exhibits a slightly faster overall decay than that observed for the isolated NCs, indicating accelerated charge recombination with no evidence of a long-lived charge separated state. (See Figure S1 for TRPL, which supports the accelerated recombination.) However, when dicyclohexylamine (**3**) is also present, in addition to octanal (sample **D**), a charge transfer behavior similar to that found in **B** is

https://dx.doi.org/10.1021/acsenergylett.9b02714
ACS Energy Lett. 2020, 5, 566−571

observed, with a faster decay in the ∼70 ps time frame followed by a much slower decay (microsecond time frame), indicating a rapid charge transfer to a charge separated state. The addition of cocatalyst (**3**) induces a charge transfer process from NCs to reactants. To further study this effect, we compare the normalized transient kinetics for **A**, with that of the NCs in the presence of just the cocatalyst (**E**) and the results are shown in Figure 2d. The transient kinetics for **E** shows an initial faster decay of around ∼70 ps followed by a much slower decay in the microsecond time frame, indicating a charge transfer between NCs and the cocatalyst.

The type of CT (electron or hole) can be studied with cyclovoltammetry (CV). The valence band and conduction band position of the NCs, taken from the literature,[33] are +1.1 and −1.3 V vs SCE (Figure 3, close to Ru based catalyst

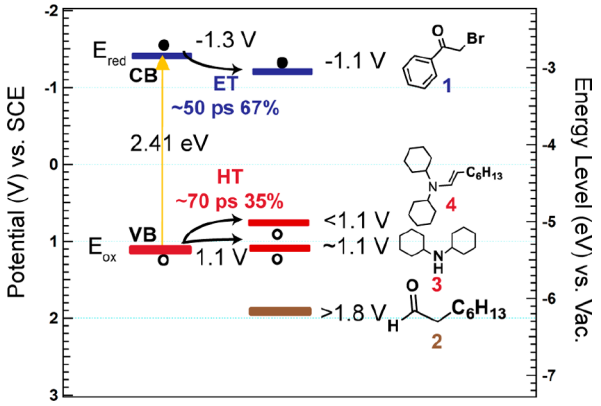

Figure 3. Electrochemical potential and energy level for NCs and reactants.

($Ru(bpy)_3^{2+}$) used in similar systems.[12] Therefore, 2-bromoacetophenone (**1**) can accept photoexcited electrons (−1.1 V vs SCE, Figure S2), octanal (**2**) should not react (1.8 V vs SCE, Figure S3), and *in-situ* formed enamine (**4**) and dicyclohexylamine (**3**) can both accept holes from the photoexcited NCs (<1.1 V vs SCE for **3**, Figure S4). Redox potential determination of the exact *in-situ* formed enamine structure was not successful, via CV, due to its transient nature. However, previous studies have suggested the hole transfer can occur from $Ru(bpy)_3^{2+}$ to the enamine.[13] Since $Ru(bpy)_3^{2+}$ has band positions similar to those of the perovskite NCs,[12] we suspect, in the actual reaction mixture, photoexcited holes can transfer from the NCs to either the amine cocatalyst or the *in-situ* formed enamine.

To quantitatively determine the dynamics of CT (ET and HT), we perform kinetic analysis with exponential fittings for the TA data. The TA kinetics can be described with three parallel processes in eq I (see the Supporting Information):

$$[N(t)] = -A_1 \cdot e^{-t/\tau_1} - A_2 \cdot e^{-t/\tau_2} - A_3 \cdot e^{-t/\tau_3} \quad \text{(I)}$$

where $N(t)$ is the exciton population at a pump−probe delay of t, τ_1, τ_2, and τ_3 are the three processes that describe charge recombination of the NCs.[34] For isolated NCs, the best-fit time constants are 260 ± 15 ps, 5.9 ± 0.3 ns, and 210 ± 19 ns, which correspond to surface trapping (260 ps) and radiative recombination (5.9 and 210 ns), respectively (see the Supporting Information, Table S1).[35] When charge transfer occurs, we introduce a term to describe the fraction of nanocrystals (f_2) that undergo charge transfer and subsequent charge separation. Due to the heterogeneous nature of the reaction, some NCs might not have electron/hole acceptors nearby and therefore this fraction (f_1) remains unchanged (see the Supporting Information and Figure S5). Thus, eq I can be rewritten as follows:

$$[N(t)] = f_1(-A_1 \cdot e^{-t/\tau_1} - A_2 \cdot e^{-t/\tau_2} - A_3 \cdot e^{-t/\tau_3}) + f_2(-B_1 \cdot e^{-t/\tau_4} - B_2 \cdot e^{-t/\tau_5}) \quad \text{(II)}$$

Here τ_4 is charge transfer time and τ_5 is charge separated state lifetime. The fitting results are shown in Figure 2c, and the best-fit parameters are listed in Table 1. In colloidal systems,

Table 1. Best Fit Parameters for NCs with 2-Bromoacetophenone and Octanal + Dicyclohexylamine

reactants	τ_4 (ps)	τ_5 (μs)	f_2 (%)
2-bromoacetophenone	50 ± 3	0.79 ± 0.03	67 ± 2
octanal + dicyclohexylamine	72 ± 7	0.53 ± 0.03	34 ± 2

characteristic charge transfer times from the NCs to molecules can span from a few picoseconds to a few nanoseconds.[27,36,37] Therefore, we assign the 50 ± 3 (ET) and 72 ± 7 ps (HT) time constants to an ultrafast charge transfer from $CsPbBr_3$ NCs to the reactants when combined with band alignment in Figure 3. Possibly, the charge transfer observed here is an outer sphere charge transfer from the NCs to molecules in solution. If the molecule is directly anchored on the NCs surface, the charge transfer can be as fast as a few picoseconds.[19,27] The 0.79 ± 0.03 and 0.53 ± 0.03 μs time constants represent the lifetimes of the charge separated state in the electron and hole acceptor as the result of the initial ET and HT, respectively.

NCs only in the presence of octanal (Figure 2c, **C** (blue curve)) did not exhibit a longer separated lifetime but a slightly shorter lifetime in the microsecond region when compared with the case for **D** (green curve). Thus, octanal does not accept holes in the absence of the cocatalyst but, rather, likely promotes surface ligand desorption, increasing the non-radiative surface defect mediated carrier recombination. As mentioned above, the HT process can occur either between the NCs and the cocatalyst (cyan curve in Figure 2d) or between the NCs and the *in-situ* formed enamine. We find here that both are able to accept holes. However, it is likely that a hole transfer to the cocatalyst will not produce the desired intermediate (i.e., oxidized enamine) and, thus, is not a desirable pathway. Therefore, the *in-situ* formed enamine should be in large abundance during the reaction.

On the basis of our TA results and intermediate lifetime, we investigated the possible mechanisms of this NCs based photocatalytic system. Several mechanisms are proposed in the literature for Ru based molecular photocatalytic systems. MacMillan[12,18,38] proposed a radical mechanism where the alkyl radical from the initial electron transfer reacts with a neutral enamine to form the C−C bond (Figure 4 dashed arrow). Then the adduct is oxidized by the photocatalyst to complete the reaction. Later, Melchiorre[39] proposed a biradical mechanism where photoexcitation generates both an alkyl and enamine radical. The two radicals then form the C−C bond and release the product, regenerating the cocatalyst. Recently, Yoon[13] and Melchiorre[40] proposed a chain reaction mechanism where the alkyl radical initiates a chain reaction by reacting with the enamine. The adduct then reacts with another neutral alkyl halide to form the product and releases

https://dx.doi.org/10.1021/acsenergylett.9b02714
ACS Energy Lett. 2020, 5, 566−571

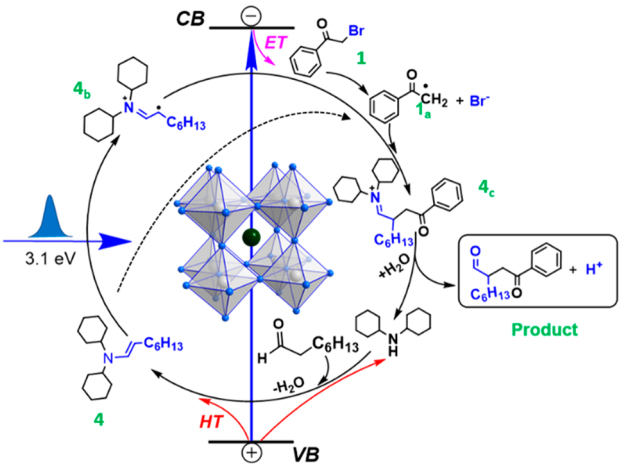

Figure 4. Proposed reaction mechanism for α-alkylation catalyzed by $CsPbBr_3$ NCs. Photogenerated electrons transfer from $CsPbBr_3$ to 2-bromoacetophenone and release bromine anions to form the radical 1_a. Photogenerated holes transfer to *in-situ* formed enamine to form radical cation 4_b. 4_b then reacts with 1_a through radical−radical coupling to form a C−C bond intermediate 4_c. The radical 1_a can also react with neutral 4 to form structure similar to 4_c and then that can accept a hole to form 4_c (depicted as the dashed arrow). Hydrolysis of 4_c leads to the product and regeneration of cocatalyst. Radical trapping experiments further confirm the formation of a radical from 2-bromoacetophenone and radical cations from enamine (Figures S6 and S7).

the alkyl radical to propagate the chain. This process can repeat for multiple cycles until the initiator is quenched. The key differentiation in these proposed mechanisms is the quantum yield of the reaction.[40] Radical and biradical mechanisms often generate relatively low quantum yields (defined here as the per photon-to-product yield <10%) as one input photon can only generate at most one C−C bond. However, chain mechanisms can often produce much higher quantum yields (often over 100%) as the chain can propagate many times and one photon can generate multiple C−C bonds and has been noted to be as high as 1800% for alkylation reactions[13,41] (meaning that one-photon yields 18 C−C bonds). Employing the methodology developed in a similar heterogeneous NCs photocatalytic system,[15] we found that the quantum yield in our system is close to 0.2% (see the Supporting Information). Such a low quantum yield suggests but does not prove that the radical or biradical mechanism dominates for these NCs based photocatalysis.

We can also use the lifetime of the reaction intermediates and known diffusion constants of the reactants to further analyze the reaction mechanism (see the Supporting Information, Figures S8−S13). In our estimate, if the substrates 2-bromoacetaphenone (**1**) and enamine (**4**) are both close to a single NC photocatalyst such that they both interact with the photoexcited NC to produce the two radicals, the average diffusion length between them will be close to 24 nm (see the Supporting Information). The diffusion constant (D) for molecules with similar structure in toluene is close to 10^{-5} cm^2 s^{-1}.[42] Since radical−radical coupling is very efficient, the estimated time for the two intermediates to meet and form a C−C bond is $\tau = \frac{L^2}{D} \sim 0.6\ \mu s$ using a 1-dimensional diffusion model. Then, the quantum yield can be calculated as percentage of charge transfer times the percentage of remaining intermediates at 0.6 μs delay. The analysis gives 11%, 30%, and 1235% for biradical, 1 cycle radical mechanism, and 40 cycles of chain propagation, respectively (see the Supporting Information).

Taking another scenario, substrate (**1**) is close to one NC while (**4**) is free or near another NC in solution, such that the photo redox species reside near separate NCs, giving an average diffusion length of 38.2 nm and corresponding reaction time of 1.4 μs. The calculated quantum yields are then 0%, 1.9%, and 448% for biradical, 1 cycle radical mechanism, and 40 cycles of chain propagation (see the Supporting Information). Therefore, with the low quantum yield experimentally observed, we believe that the reaction in our perovskite NCs likely proceeds *via* the biradical or 1 cycle radical mechanism rather than a chain propagation. Note that the chain mechanism is just the radical mechanism that is allowed to propagate. Another argument in support of the proposed biradical mechanism is that we observe a very efficient ultrafast hole transfer to the enamine. However, solely on the basis of our lifetime data, we cannot rule out the radical mechanism and both pathways can likely occur simultaneously. The primary difference between the molecular system and NCs is that in $Ru(bpy)_3^{2+}$ based systems, the excited state lifetime can be very long (10 μs),[43] allowing the chain to propagate. However, in the NCs system, the excited state lifetime is shorter and only the biradical or 1 cycle radical mechanisms can occur prior to deactivation of the catalyst.

We then propose the following reaction pathway (Figure 4). After photoexcitation, electron transfer (ET) to 2-bromoacetophenone is within 50 ps, reducing it to its radical anion, which immediately dissociates into its radical ($\mathbf{1_a}$) and a bromine anion. Meanwhile, there is a ∼70 ps photoexcited hole transfer from the NCs to the *in-situ* formed enamine (which is formed by the cocatalyst dicyclohexylamine and the reactant octanal with the loss of water) or the hole can also transfer to the cocatalyst dicyclohexylamine. The hole transfer to the enamine will result in the formation of the radical cation intermediate $\mathbf{4_b}$. The radical cation $\mathbf{4_b}$ can react with the radical $\mathbf{1_a}$ to form the intermediate $\mathbf{4_c}$ (biradical mechanism). Potentially, **1a** can also react with **4** to form a structure that is similar to **4c**,(1 cycle radical mechanism) which accepts a hole to form **4c**. **4c** then reacts with transient water (probably from enamine formation) to release the final product and a proton, along with regenerating the cocatalyst (dicyclohexylamine). The base, 2,6-lutidine, neutralizes HBr.

In conclusion, we have observed ultrafast electron transfer (∼50 ps) from $CsPbBr_3$ NCs to 2-bromoacetophenone and hole transfer (∼70 ps) to an *in-situ* formed enamine or cocatalyst. As a result of this charge transfer, a charge separated state with ∼0.8 μs lifetime is formed. This near microsecond charge separated state allows the photogenerated charged radical intermediates to form a C−C bond in a biradical pathway but does not allow the chain to propagate. The primary difference between the NCs photoredox catalysts studied here and the molecular catalyst is the lifetime of the charge separated state.

■ ASSOCIATED CONTENT

Supporting Information

The Supporting Information is available free of charge at https://pubs.acs.org/doi/10.1021/acsenergylett.9b02714.

Perovskite NCs synthesis, TA experiment setup, exciton number calculation, TA and TRPL dynamics with

https://dx.doi.org/10.1021/acsenergylett.9b02714
ACS Energy Lett. 2020, 5, 566−571

different substrates, CVs of reactant molecules, kinetics analysis with a table of fitted time constants, radical trapping reactions with LC−MS spectra, quantum yield calculation, reaction mechanism discussion with reaction diagrams (PDF)

AUTHOR INFORMATION

Corresponding Authors

Matthew C. Beard − *Chemistry and Nano Science Center, National Renewable Energy Laboratory, Golden, Colorado 80401, United States;* orcid.org/0000-0002-2711-1355; Email: Matt.Beard@nrel.gov

Yong Yan − *Department of Chemistry, San Diego State University, San Diego, California 92182, United States;* orcid.org/0000-0001-6361-0541; Email: Yong.yan@sdsu.edu

Xihan Chen − *Chemistry and Nano Science Center, National Renewable Energy Laboratory, Golden, Colorado 80401, United States;* orcid.org/0000-0001-7907-2549; Email: Xihan.Chen@nrel.gov

Authors

Kang Wang − *State Key Laboratory of Physical Chemistry of Solid Surfaces, College of Chemistry and Chemical Engineering, Xiamen University, Xiamen 361005, China; Chemistry and Nano Science Center, National Renewable Energy Laboratory, Golden, Colorado 80401, United States*

Haipeng Lu − *Chemistry and Nano Science Center, National Renewable Energy Laboratory, Golden, Colorado 80401, United States;* orcid.org/0000-0003-0252-3086

Xiaolin Zhu − *Department of Chemistry, San Diego State University, San Diego, California 92182, United States;* orcid.org/0000-0001-6568-0308

Yixiong Lin − *Department of Chemistry, San Diego State University, San Diego, California 92182, United States*

Complete contact information is available at: https://pubs.acs.org/10.1021/acsenergylett.9b02714

Author Contributions

#K.W., H.L., and X.Z. contributed equally to this work.

Notes

The authors declare no competing financial interest.

ACKNOWLEDGMENTS

We gratefully acknowledge the support from the Center for Hybrid Organic Inorganic Semiconductors for Energy (CHOISE), an Energy Frontier Research Center funded by the Office of Basic Energy Sciences, Office of Science, within the U.S. Department of Energy through contract number DE-AC36-08GO28308 with NREL. The views expressed in the Letter do not necessarily represent the views of the DOE or the U.S. Government. The U.S. Government retains and the publisher, by accepting the article for publication, acknowledges that the U.S. Government retains a nonexclusive, paid-up, irrevocable, worldwide license to publish or reproduce the published form of this work, or allow others to do so, for U.S. Government purposes. Y.Y. acknowledges partial support from NSF under CHE-1851747 in determining the C−C bond formation yields. K.W. acknowledges fellowship suport from the China Scholarship Council and National Natural Scicence Foundations of China (21973078). The authors thanks Ye Yang and Yaxin Zhai for fruitful discussions.

REFERENCES

(1) Lewis, N. S.; Nocera, D. G. Powering the planet: Chemical challenges in solar energy utilization. *Proc. Natl. Acad. Sci. U. S. A.* **2006**, *103* (43), 15729.

(2) Nozik, A. J.; Miller, J. Introduction to Solar Photon Conversion. *Chem. Rev.* **2010**, *110* (11), 6443−6445.

(3) Kamat, P. V.; Jin, S. Semiconductor Photocatalysis: "Tell Us the Complete Story! *ACS Energy Lett.* **2018**, *3* (3), 622−623.

(4) Zhang, Z.; Edme, K.; Lian, S.; Weiss, E. A. Enhancing the Rate of Quantum-Dot-Photocatalyzed Carbon−Carbon Coupling by Tuning the Composition of the Dot's Ligand Shell. *J. Am. Chem. Soc.* **2017**, *139* (12), 4246−4249.

(5) Caputo, J. A.; Frenette, L. C.; Zhao, N.; Sowers, K. L.; Krauss, T. D.; Weix, D. J. General and Efficient C−C Bond Forming Photoredox Catalysis with Semiconductor Quantum Dots. *J. Am. Chem. Soc.* **2017**, *139* (12), 4250−4253.

(6) McClelland, K. P.; Weiss, E. A. Selective Photocatalytic Oxidation of Benzyl Alcohol to Benzaldehyde or C−C Coupled Products by Visible-Light-Absorbing Quantum Dots. *ACS Appl. Energy Mater.* **2019**, *2* (1), 92−96.

(7) Ponseca, C. S.; Chábera, P.; Uhlig, J.; Persson, P.; Sundström, V. Ultrafast Electron Dynamics in Solar Energy Conversion. *Chem. Rev.* **2017**, *117* (16), 10940−11024.

(8) Chen, X.; Wang, K.; Beard, M. C. Ultrafast probes at the interfaces of solar energy conversion materials. *Phys. Chem. Chem. Phys.* **2019**, *21* (30), 16399−16407.

(9) Bushuyev, O. S.; De Luna, P.; Dinh, C. T.; Tao, L.; Saur, G.; van de Lagemaat, J.; Kelley, S. O.; Sargent, E. H. What Should We Make with CO2 and How Can We Make It? *Joule* **2018**, *2* (5), 825−832.

(10) Chen, X.; Choing, S. N.; Aschaffenburg, D. J.; Pemmaraju, C. D.; Prendergast, D.; Cuk, T. The Formation Time of Ti-O(*) and Ti-O(*)-Ti Radicals at the n-$SrTiO_3$/Aqueous Interface during Photocatalytic Water Oxidation. *J. Am. Chem. Soc.* **2017**, *139* (5), 1830−1841.

(11) Chen, X.; Aschaffenburg, D. J.; Cuk, T. Selecting between two transition states by which water oxidation intermediates decay on an oxide surface. *Nat. Catal.* **2019**, *2* (9), 820−827.

(12) Nicewicz, D. A.; MacMillan, D. W. C. Merging Photoredox Catalysis with Organocatalysis: The Direct Asymmetric Alkylation of Aldehydes. *Science* **2008**, *322* (5898), 77.

(13) Cismesia, M. A.; Yoon, T. P. Characterizing chain processes in visible light photoredox catalysis. *Chem. Sci.* **2015**, *6* (10), 5426−5434.

(14) Zhu, X.; Lin, Y.; Sun, Y.; Beard, M. C.; Yan, Y. Lead-Halide Perovskites for Photocatalytic α-Alkylation of Aldehydes. *J. Am. Chem. Soc.* **2019**, *141* (2), 733−738.

(15) Zhu, X.; Lin, Y.; San Martin, J.; Sun, Y.; Zhu, D.; Yan, Y. Lead halide perovskites for photocatalytic organic synthesis. *Nat. Commun.* **2019**, *10* (1), 2843.

(16) Lu, H.; Zhu, X.; Miller, C.; San Martin, J.; Chen, X.; Miller, E. M.; Yan, Y.; Beard, M. C. Enhanced photoredox activity of CsPbBr3 nanocrystals by quantitative colloidal ligand exchange. *J. Chem. Phys.* **2019**, *151* (20), 204305.

(17) Prier, C. K.; Rankic, D. A.; MacMillan, D. W. C. Visible Light Photoredox Catalysis with Transition Metal Complexes: Applications in Organic Synthesis. *Chem. Rev.* **2013**, *113* (7), 5322−5363.

(18) Twilton, J.; Le, C.; Zhang, P.; Shaw, M. H.; Evans, R. W.; MacMillan, D. W. C. The merger of transition metal and photocatalysis. *Nat. Rev. Chem.* **2017**, *1* (7), 0052.

(19) Lu, H.; Chen, X.; Anthony, J. E.; Johnson, J. C.; Beard, M. C. Sensitizing Singlet Fission with Perovskite Nanocrystals. *J. Am. Chem. Soc.* **2019**, *141* (12), 4919−4927.

(20) He, S.; Luo, X.; Liu, X.; Li, Y.; Wu, K. Visible-to-Ultraviolet Upconversion Efficiency above 10% Sensitized by Quantum-Confined Perovskite Nanocrystals. *J. Phys. Chem. Lett.* **2019**, *10* (17), 5036−5040.

(21) Han, Y.; Luo, X.; Lai, R.; Li, Y.; Liang, G.; Wu, K. Visible-Light-Driven Sensitization of Naphthalene Triplets Using Quantum-

Confined CsPbBr3 Nanocrystals. *J. Phys. Chem. Lett.* **2019**, *10* (7), 1457−1463.
(22) Luo, X.; Lai, R.; Li, Y.; Han, Y.; Liang, G.; Liu, X.; Ding, T.; Wang, J.; Wu, K. Triplet Energy Transfer from CsPbBr3 Nanocrystals Enabled by Quantum Confinement. *J. Am. Chem. Soc.* **2019**, *141* (10), 4186−4190.
(23) Kodaimati, M. S.; McClelland, K. P.; He, C.; Lian, S.; Jiang, Y.; Zhang, Z.; Weiss, E. A. Viewpoint: Challenges in Colloidal Photocatalysis and Some Strategies for Addressing Them. *Inorg. Chem.* **2018**, *57* (7), 3659−3670.
(24) Weiss, E. A. Designing the Surfaces of Semiconductor Quantum Dots for Colloidal Photocatalysis. *ACS Energy Lett.* **2017**, *2* (5), 1005−1013.
(25) Jiang, Y.; Wang, C.; Rogers, C. R.; Kodaimati, M. S.; Weiss, E. A. Regio- and diastereoselective intermolecular [2 + 2] cycloadditions photocatalysed by quantum dots. *Nat. Chem.* **2019**, *11* (11), 1034−1040.
(26) Cottingham, P.; Brutchey, R. L. On the crystal structure of colloidally prepared CsPbBr3 quantum dots. *Chem. Commun.* **2016**, *52* (30), 5246−5249.
(27) Wu, K.; Liang, G.; Shang, Q.; Ren, Y.; Kong, D.; Lian, T. Ultrafast Interfacial Electron and Hole Transfer from CsPbBr3 Perovskite Quantum Dots. *J. Am. Chem. Soc.* **2015**, *137* (40), 12792−12795.
(28) Lu, H.; Carroll, G. M.; Chen, X.; Amarasinghe, D. K.; Neale, N. R.; Miller, E. M.; Sercel, P. C.; Rabuffetti, F. A.; Efros, A. L.; Beard, M. C. n-Type PbSe Quantum Dots via Post-Synthetic Indium Doping. *J. Am. Chem. Soc.* **2018**, *140* (42), 13753−13763.
(29) Chen, X.; Lu, H.; Li, Z.; Zhai, Y.; Ndione, P. F.; Berry, J. J.; Zhu, K.; Yang, Y.; Beard, M. C. Impact of Layer Thickness on the Charge Carrier and Spin Coherence Lifetime in Two-Dimensional Layered Perovskite Single Crystals. *ACS Energy Lett.* **2018**, *3* (9), 2273−2279.
(30) Chen, X.; Lu, H.; Yang, Y.; Beard, M. C. Excitonic Effects in Methylammonium Lead Halide Perovskites. *J. Phys. Chem. Lett.* **2018**, *9* (10), 2595−2603.
(31) Zhu, H.; Yang, Y.; Wu, K.; Lian, T. Charge Transfer Dynamics from Photoexcited Semiconductor Quantum Dots. *Annu. Rev. Phys. Chem.* **2016**, *67* (1), 259−281.
(32) Luo, X.; Liang, G.; Wang, J.; Liu, X.; Wu, K. Picosecond multi-hole transfer and microsecond charge-separated states at the perovskite nanocrystal/tetracene interface. *Chem. Sci.* **2019**, *10* (8), 2459−2464.
(33) Ravi, V. K.; Markad, G. B.; Nag, A. Band Edge Energies and Excitonic Transition Probabilities of Colloidal CsPbX3 (X = Cl, Br, I) Perovskite Nanocrystals. *ACS Energy Lett.* **2016**, *1* (4), 665−671.
(34) Koscher, B. A.; Swabeck, J. K.; Bronstein, N. D.; Alivisatos, A. P. Essentially Trap-Free CsPbBr3 Colloidal Nanocrystals by Postsynthetic Thiocyanate Surface Treatment. *J. Am. Chem. Soc.* **2017**, *139* (19), 6566−6569.
(35) Li, B.; Huang, H.; Zhang, G.; Yang, C.; Guo, W.; Chen, R.; Qin, C.; Gao, Y.; Biju, V. P.; Rogach, A. L.; Xiao, L.; Jia, S. Excitons and Biexciton Dynamics in Single CsPbBr3 Perovskite Quantum Dots. *J. Phys. Chem. Lett.* **2018**, *9* (24), 6934−6940.
(36) Mandal, S.; George, L.; Tkachenko, N. V. Charge transfer dynamics in CsPbBr3 perovskite quantum dots−anthraquinone/fullerene (C60) hybrids. *Nanoscale* **2019**, *11* (3), 862−869.
(37) Kobosko, S. M.; DuBose, J. T.; Kamat, P. V. Perovskite Photocatalysis. Methyl Viologen Induces Unusually Long-Lived Charge Carrier Separation in CsPbBr3 Nanocrystals. *ACS Energy Lett.* **2020**, *5* (1), 221−223.
(38) Welin, E. R.; Warkentin, A. A.; Conrad, J. C.; MacMillan, D. W. C. Enantioselective α-Alkylation of Aldehydes by Photoredox Organocatalysis: Rapid Access to Pharmacophore Fragments from β-Cyanoaldehydes. *Angew. Chem., Int. Ed.* **2015**, *54* (33), 9668−9672.
(39) Arceo, E.; Jurberg, I. D.; Álvarez-Fernández, A.; Melchiorre, P. Photochemical activity of a key donor−acceptor complex can drive stereoselective catalytic α-alkylation of aldehydes. *Nat. Chem.* **2013**, *5* (9), 750−756.
(40) Bahamonde, A.; Melchiorre, P. Mechanism of the Stereoselective α-Alkylation of Aldehydes Driven by the Photochemical Activity of Enamines. *J. Am. Chem. Soc.* **2016**, *138* (25), 8019−8030.
(41) Silvi, M.; Arceo, E.; Jurberg, I. D.; Cassani, C.; Melchiorre, P. Enantioselective Organocatalytic Alkylation of Aldehydes and Enals Driven by the Direct Photoexcitation of Enamines. *J. Am. Chem. Soc.* **2015**, *137* (19), 6120−6123.
(42) Saiki, H.; Takami, K.; Tominaga, T. Diffusion of porphyrins and quinones in organic solvents. *Phys. Chem. Chem. Phys.* **1999**, *1* (2), 303−306.
(43) Crosby, G. A.; Demas, J. N. Quantum efficiencies on transition metal complexes. II. Charge-transfer luminescence. *J. Am. Chem. Soc.* **1971**, *93* (12), 2841−2847.

https://dx.doi.org/10.1021/acsenergylett.9b02714
ACS Energy Lett. 2020, 5, 566−571